Single Photon Ionization and Chemical Ionization Combined Ion Source Based on a Vacuum Ultraviolet Lamp for Orthogonal Acceleration Time-of-Flight Mass Spectrometry

ARTICLE *in* ANALYTICAL CHEMISTRY · JUNE 2011

Impact Factor: 5.64 · DOI: 10.1021/ac200742r · Source: PubMed

8 AUTHORS, INCLUDING:

Lei Hua
Dalian Institute of Chemical Physics
29 PUBLICATIONS **119** CITATIONS
SEE PROFILE

Keyong Hou
Dalian Institute of Chemical Physics
53 PUBLICATIONS **272** CITATIONS
SEE PROFILE

Weiguo Wang
Dalian Institute of Chemical Physics
38 PUBLICATIONS **240** CITATIONS
SEE PROFILE

Jinghua Li
Chinese Academy of Sciences
11 PUBLICATIONS **100** CITATIONS
SEE PROFILE

analytical chemistry

ARTICLE

pubs.acs.org/ac

Single Photon Ionization and Chemical Ionization Combined Ion Source Based on a Vacuum Ultraviolet Lamp for Orthogonal Acceleration Time-of-Flight Mass Spectrometry

Lei Hua,[†,‡] Qinghao Wu,[†,‡] Keyong Hou,[*,†] Huapeng Cui,[†,‡] Ping Chen,[†,‡] Weiguo Wang,[†] Jinghua Li,[†] and Haiyang Li[*,†]

[†]Dalian Institute of Chemical Physics, Chinese Academy of Sciences, Dalian 116023, People's Republic of China

[‡]Graduate School of Chinese Academy of Sciences, Beijing 100039, People's Republic of China

Supporting Information

ABSTRACT: A novel combined ion source based on a vacuum ultraviolet (VUV) lamp with both single photon ionization (SPI) and chemical ionization (CI) capabilities has been developed for an orthogonal acceleration time-of-flight mass spectrometer (oaTOFMS). The SPI was accomplished using a commercial 10.6 eV krypton discharge lamp with a photon flux of about 10^{11} photons s^{-1}, while the CI was achieved through ion−molecule reactions with O_2^+ reactant ions generated by photoelectron ionization at medium vacuum pressure (MVP). To achieve high ionization efficiency, the ion source pressure was elevated to 0.3 mbar and the photoionization length was extended to 36 mm. As a result, limits of detection (LODs) down to 3, 4, and 6 ppbv were obtained for benzene, toluene, and *p*-xylene in MVP-SPI mode, and values of 8 and 10 ppbv were obtained for toluene and chloroform, respectively, in SPI-CI mode. As it is feasible to switch between MVP-SPI mode and SPI-CI mode rapidly, this system is capable of monitoring complex organic mixtures with a wide range of ionization energies (IEs). The analytical capacity of this system was demonstrated by measuring dehydrogenation products of long-chain paraffins to olefins through direct capillary sampling and drinking water disinfection byproducts from chlorine through a membrane interface.

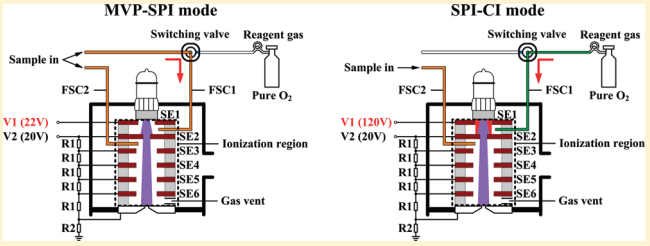

Single photon ionization (SPI) is characterized by its high molecular ion yield and very low degree of fragmentation, when compared with other ionization methods, such as 70 eV electron impact (EI) ionization.[1−6] The coupling of SPI and mass spectrometry (MS) has attracted great attention for online and in situ analysis of organic species in recent years.[7−13]

Most of the current SPI sources used in mass spectrometry systems are operated at high vacuum pressures (below 10^{-3} mbar).[14−16] Because the ionization cross sections for SPI of common organic compounds are typically 2 orders of magnitude lower than that for 70 eV EI, the ionization efficiency of SPI is relatively low compared to that of EI at similar conditions. Therefore, the photon flux of vacuum ultraviolet (VUV) light sources is crucial to the current SPI ion sources for high-sensitivity SPI-MS analysis. The commercial low pressure discharge lamps filled with various rare gases, such as krypton discharge lamps, are compact and low cost and have been utilized in SPI-MS for online monitoring of volatile organic compounds (VOCs).[17,18] However, the relatively low photon intensity of these lamps limits their applications in current SPI-MS systems. Efforts have been taken to develop stronger VUV light sources to solve this issue. Laser-based sources and high-intensity VUV lamps, such as Nd:YAG laser based sources,[19,20] a hydrogen Lyman-α atomic radiation based microwave discharge lamp,[21] and an electron beam pumped rare gas excimer lamp (EBEL),[22,23] have been employed in SPI-MS for sensitivity improvement. However, the laser based sources require expensive, bulky, and complicated laser devices, and high-intensity VUV lamps are limited to lab applications, because of their size. The lack of commercial products of affordable and compact high-intensity VUV sources has been a bottleneck for further development of the current SPI-MS systems, especially for in situ applications.

Fortunately, improving the light intensity of VUV light sources is not the only way to realize high-sensitivity SPI-MS analysis. The production rate I_{SPI} (ions s^{-1}) of the ions in an SPI process can be expressed as follows (the derivation can be found in the Supporting Information):

$$I_{SPI} = \sigma_{PI} I_0 N L \quad (1)$$

where σ_{PI} (Mb, 1Mb = 10^{-18} cm^2) is the photoionization cross section of the analyte, I_0 (photons s^{-1}) is the light intensity of the VUV source, N (cm^{-3}) is the molecular number density of the

Received: March 24, 2011
Accepted: May 18, 2011
Published: May 18, 2011

analyte, and L (cm) is the photoionization length. Therefore, increasing the number density of the analytes in the ionization region and lengthening the photoionization length can also effectively improve the sensitivity of SPI-MS. In direct-sampling MS systems, the number density of the analyte in the ion source region can be increased by elevating the ion source pressure. Syage et al.[24,25] constructed a low pressure photoionization (LPPI) source (1.33−5.32 mbar) using an RF discharge lamp for a portable quadrupole ion trap/time-of-flight (QITTOF) MS. For chemical-weapons-related compounds, the limits of detection (LODs) of this system ranged from 10 to 100 ppbv. Further pressure increase in the ion source region will turn SPI to atmospheric pressure photon ionization (APPI). At atmospheric pressure, the VUV photon beam intensity drops by half each 1.5 mm,[26] so the effective ionization length of VUV photons is limited to several millimeters. The ionization probability for SPI of analyte molecules is very low because of the trace concentration.[27] To increase the ionization efficiency of analyte molecules, varieties of dopants are usually added to react with the analyte molecules through ion−molecule reactions.[28−30] However, ion−molecule reactions, such as charge transfer and proton transfer in APPI, are combined with the problem of matrix effects.[31,32]

Molecules with ionization energies (IEs) higher than the photon energy (e.g., 10.6 eV for VUV lamp) cannot be ionized by SPI. Some organic pollutants in the environment, such as methane (CH_4, IE = 12.61 eV),[33] acetonitrile (CH_3CN, IE = 12.20 eV),[33] and some halogenated hydrocarbons, are not observable in most SPI mass spectra. To address this problem, Zimmermann et al.[22] designed a combined ion source coupling of EBEL-SPI and conventional EI, which was capable of producing both SPI and EI mass spectra with good detection efficiencies. The LODs of SPI and EI for toluene were found to be 35 and 700 ppbv, respectively. However, the pressure in the ion source region must be kept low enough to protect the heated filament, which leads to low molecular density of analytes in the ion source region and consequently restricts further improvement of the sensitivity. Several laser-induced photoelectron ionization sources have been constructed with the advantage of working at a wider pressure range over heated filaments.[34−39] However, the complexity and high cost of laser devices limit their utility in practical applications. Zenobi et al.[40] and Li et al.[18] recently presented a photoelectron ionization source using a commercial VUV discharge lamp as the light source. Molecules with IEs higher than the photon energy were ionized by photoelectron ionization, and the resultant mass spectra had fragmentation patterns similar to those of EI. Moreover, this photoelectron ionization method can work at relatively high ion source pressure up to 10^{-3} mbar.

In this study, we introduced a new ion source with both medium vacuum pressure SPI (MVP-SPI) and chemical ionization (CI) capabilities for an orthogonal acceleration time-of-flight mass spectrometer (oaTOFMS), using a commercial 10.6 eV VUV lamp. The ion source pressure was elevated to medium vacuum pressure (10^{-3} to 1 mbar), and the photoionization length was increased to tens of millimeters, to improve the sensitivity of SPI-MS. The probability of CI with O_2^+ reactant ions, which are generated by photoelectron ionization of pure oxygen gas as the reagent gas, is also verified. Preliminary applications have been demonstrated by online monitoring of the dehydrogenation of long-chain paraffins and the disinfection byproducts of drinking water.

EXPERIMENTAL SECTION

Sample Preparation. A standard gas mixture containing benzene, toluene, and *p*-xylene with a respective concentration of 10 ppmv in nitrogen (Dalian Special Gas Company, Dalian, China) was used to characterize the performance of the newly developed ion source and was further diluted with pure nitrogen gas (99.999%) to the lower concentrations required. Desired concentrations of propenenitrile, toluene, and chloroform were prepared by diluting pure reagents with pure nitrogen gas, using a polytetrafluoroethylene (PTFE) sampling bag and mass flow controllers (Seven Star Electronics Co., Ltd., Beijing, China). Details of the dilution process can be found elsewhere.[17] All of the reagents used were analytical grade.

Instrumentation. The home-built mass spectrometer shown in Figure 1a consists of a VUV lamp based ion source, an electrostatic ion optics, and an oaTOF mass analyzer. Gas-phase analytes were directly introduced into the ion source through two parallel 250 μm i.d., 1 m long fused silica capillaries. The ion source was pumped by a 3.5 L/s dry scroll vacuum pump (Agilent Technologies Inc., California, U.S.A.). The electrostatic ion optics, composed of a skimmer and an einzel lens, was separated from the ion source by a sampler with a 1 mm i.d. center hole. The skimmer has a 1 mm i.d. orifice and was located 6 mm downstream of the sampler. The ion optics and the mass analyzer regions were differentially pumped by a 110 L/s and a 600 L/s turbo molecular pump (KYKY Technology Development Ltd., Beijing, China), respectively. The oaTOF mass analyzer was operated in linear mode based on the double electric field design of Wiley and McLaren.[41] The ions in the ion source were transferred through the sampler center hole and the skimmer orifice into the einzel lens, which further collimated the ion beam and guided the ions through a 2 mm × 12 mm slit into the extraction region. A 50 mm chevron MCP detector with a 50 Ω conical anode was used to collect the ions, and signals were recorded using a 100-ps time-to-digital converter (TDC) (model 9353, Ametec Inc., Oak Ridge, U.S.A.). The data were recorded with a repetition rate of 50 kHz, and all the mass spectra were accumulated for 10 s. A mass resolving power of 900 (fwhm) was achieved at m/z 78 using the oaTOFMS, which only has a 550 mm field-free flight length.

The sample inlet system and the combined ion source operated in different modes are shown in Figure 1b and c. The sample inlet system consists of a three-way ball valve (Swaglok Company, Michigan, U.S.A.) and two 250 μm i.d., 1 m long fused silica capillaries (FSC1 and FSC2). FSC1 and FSC2 were all used to introduce gas-phase samples with a gas flow rate of 30 mL/min in MVP-SPI mode, while, in SPI-CI mode, FSC1 was changed by the valve to the reagent gas of pure oxygen gas (99.999%) to produce O_2^+ reactant ions.

The ion source includes two parts: a VUV lamp and an ionization region. The commercial 10.6 eV krypton discharge lamp (Cathodeon Ltd., Cambridge, U.K.) with the photon flux of about 1×10^{11} photons s^{-1} was installed on the top of the ionization region. The ionization region with a total length of 36 mm was constructed by six 1 mm thick stainless steel electrodes (SE1−SE6), which were separated by six 5 mm thick PTFE insulation washers. A gas vent underneath the ionization region was employed for neutral gases exhausting from the ionization region into the ion source chamber. The photoionization length is defined as the distance from the VUV lamp window to the sampler, which is the length of the ionization region. The diameters of the center holes in

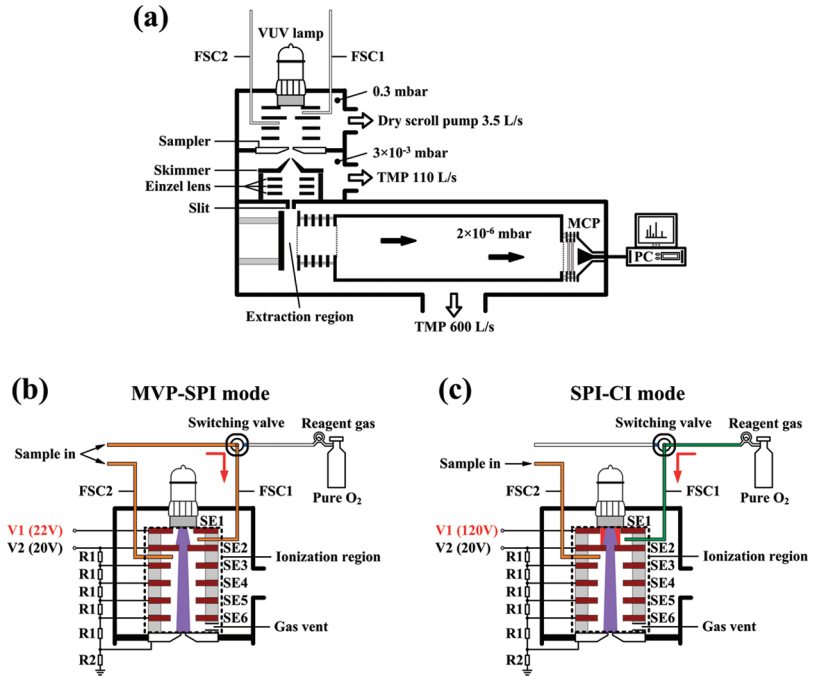

Figure 1. (a) Schematic diagram of the home-built mass spectrometer with the combined SPI and CI ion source. (b) Schematic diagram of the combined ion source operating in MVP-SPI mode. (c) Schematic diagram of the combined ion source operating in SPI-CI mode.

the electrodes are 6 mm for SE1, 3 mm for SE2, and 12 mm for SE3−SE6. The positive dc voltages applied to SE2−SE6 and the sampler were provided by a dc power supply (V2) and divided by a resistor string (R1 and R2), while the voltage of SE1 (V1) was controlled independently. The voltage of V2 and the resistances of R1 and R2 were optimized as 20 V, 1 MΩ, and 3.3 MΩ, respectively.

The ion source could work at different operation modes, the MVP-SPI and SPI-CI modes, by simply adjusting V1 and switching SFC1 to corresponding gases, as shown in Figure 1b and c. In MVP-SPI mode, V1 was set to 22 V and the gas-phase sample was selected to flow through FSC1. The photoelectrons emitted from the SE2 surface could not obtain enough energy for effective electron ionization, so the ionization process was dominated by SPI. In SPI-CI mode, V1 was set to 120 V and the reagent gas was selected to flow through FSC1. The photoelectrons emitted from the SE2 surface could obtain tens of eV energies to ionize O_2 and produce dominant O_2^+ reactant ions between SE1 and SE2. The O_2^+ reactant ions were then transferred into the ionization region between SE2 and the sampler to react with the analyte molecules. The analyte molecules with IEs higher than 10.6 eV could be ionized effectively by the CI mechanism, while the analyte molecules with IEs lower than 10.6 eV were ionized by both the SPI and CI mechanisms. Manual switching between these two modes took only a few seconds.

RESULTS AND DISCUSSION

Ion Source Pressure Effects in MVP-SPI Mode. The pressure in the ion source region was varied from 0.02 to 1 mbar by employing capillaries with different inner diameters and lengths. The length of the ionization region was fixed at 36 mm during the variation of the ion source pressure. Figure 2a shows the MVP-SPI mass spectra of 10 ppmv benzene (m/z 78, IE = 9.24 eV),[33] toluene (m/z 92, IE = 8.83 eV),[33] and *p*-xylene (m/z 106, IE = 8.44 eV)[33] at different pressures. Only molecular ions were observed in the mass spectra for each analyte. The ion peak at m/z 223 is attributed to the ionization of oil molecules evaporated from the molecular pumps. Figure 2b plots the signal intensities of toluene and the oil background versus the pressure in the ion source region. The intensities of benzene, toluene, and *p*-xylene rose rapidly as the ion source pressure was elevated from 0.02 mbar to approximately 0.3 mbar, which is attributed to the increased density of the analyte. In our direct-sampling MS system, the number density of gaseous analyte in the ionization region is directly proportional to the pressure of the ion source; thus, more analyte ions were obtained when the ion source pressure was increased from 0.02 mbar to 0.3 mbar, according to eq 1. As the pressure increased from 0.3 to 1 mbar, the ion intensities of the analytes decreased as a result of the excessive ion−molecule collisions under higher pressures. The results also suggest that high pressure in the ion source region helps to prevent the oil back-streaming from the analyzer chamber. The optimized pressure in the ion source was found to be 0.3 mbar.

Photoionization Length Effects in MVP-SPI Mode. In order to investigate the influence of the photoionization length, the ion source was designed with a slipper seal mode, as shown in Figure 3a. The VUV lamp was fixed at the end of a slide rod that was installed coaxial with the ionization region. Following the movements of the slide rod, the VUV lamp was moved along the axis direction of the ionization region to change the photoionization length. The movements of the slide rod were controlled manually outside the ion source during the experiment. The electrodes in the ionization region were enlarged to enable analyte molecules to pass through the interspaces between the electrodes and the slide rod into the ionization region.

A gas mixture of 10 ppmv benzene, toluene, and *p*-xylene was introduced into the ion source region, and the ion source pressure was maintained at 0.3 mbar during the variation of the photoionization length. Figure 3b shows the effects of the photoionization

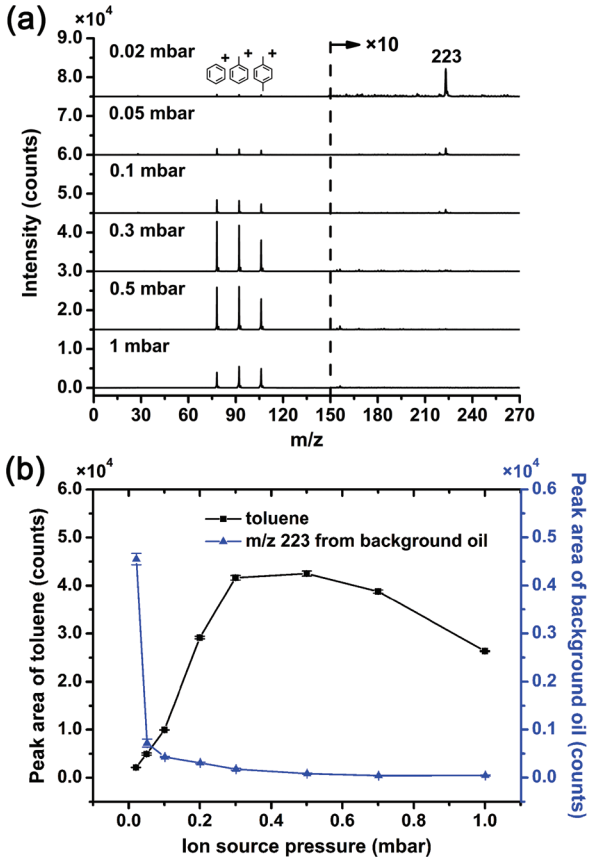

Figure 2. (a) MVP-SPI mass spectra obtained for 10 ppmv benzene, toluene, and *p*-xylene standard gas mixtures at various ion source pressures: 0.02, 0.05, 0.1, 0.3, 0.5, and 1 mbar (analysis time 10 s). (b) Peak areas of toluene (*m*/*z* 92) and background oil (*m*/*z* 223) as a function of the ion source pressure in MVP-SPI mode.

length on the signal intensities of benzene, toluene, and *p*-xylene in MVP-SPI mode. When the photoionization length was increased from 2 to 8 mm, a sharp rise in peak intensities occurred, as predicted by eq 1. The peak intensities reached their maximum values at approximately 10 mm and then declined as the photoionization length was further increased. There are two factors affecting the ionization sensitivity: the number of analyte ions and the ion transfer efficiency to the mass analyzer. Improvement in signal intensities under 10 mm photoionization length is attributed to the increase in analyte ion amount. More analyte molecules will absorb the VUV photons at the longer photoionization length and, thus, are ionized to create more analyte ions. Ions in the ion source suffer from a diffusion problem when transmitting long distance in a uniform electrostatic field, and the ion transfer efficiency will be degraded when the photoionization length is further raised above 10 mm. However, ion−molecule reactions in SPI-CI mode need more reaction space to improve its sensitivity. Therefore, to balance the sensitivity between MVP-SPI and SPI-CI, the length of the ionization region was set as 36 mm, though the MVP-SPI signal intensities at the photoionization length of 36 mm were about 40% lower than the maximum values at 10 mm.

LODs and Linear Dynamic Range in MVP-SPI Mode. Figure 4 shows the calibration curves of benzene, toluene, and *p*-xylene in MVP-SPI mode. Three orders of magnitude linear dynamic range was obtained in the concentration range from 10 ppbv to 10 ppmv with satisfactory correlation coefficients

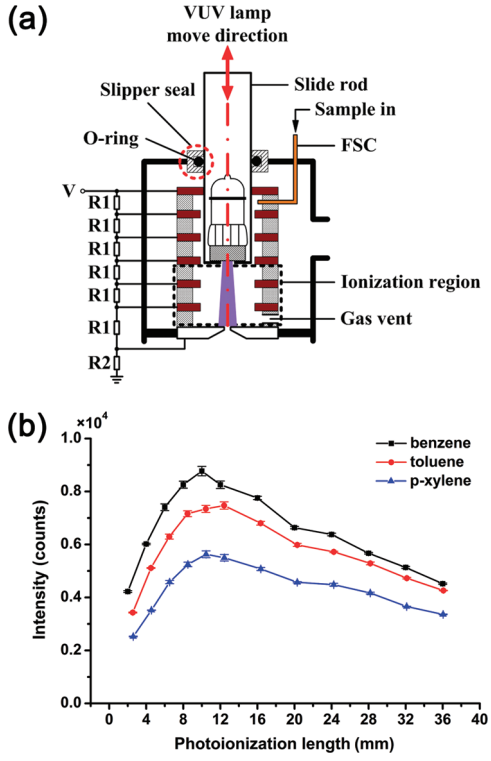

Figure 3. (a) Schematic diagram of the modified ion source with a slipper seal design. (b) Peak intensities of benzene, toluene, and *p*-xylene as a function of the photoionization length in MVP-SPI mode.

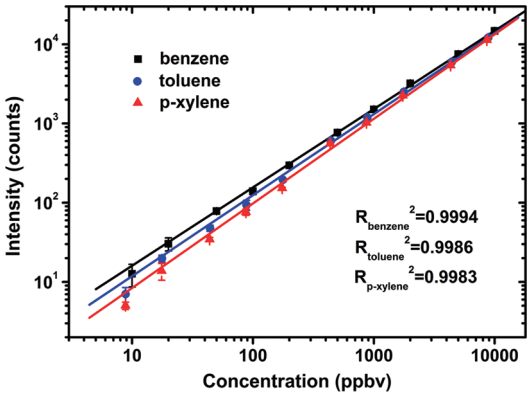

Figure 4. Linear calibration curves for benzene, toluene, and *p*-xylene gas mixtures in the concentration range from 10 ppbv to 10 ppmv in MVP-SPI mode.

($R_{benzene}^2 = 0.9994$, $R_{toluene}^2 = 0.9986$, $R_{p\text{-}xylene}^2 = 0.9983$). Based on the S/N = 3 criteria, the LODs for benzene, toluene, and *p*-xylene in MVP-SPI mode were calculated to be 3, 4, and 6 ppbv, within 10 s analysis time, respectively. The MVP-SPI shows a great advantage over the high vacuum pressure SPI. The sensitivity is improved by about 30-fold compared to our previous result,[18] which was recorded at the ion source pressure of 2×10^{-3} mbar using the same VUV light source, and is about 1 order of magnitude higher than that obtained by an EBEL even with the photon flux of 1.5×10^{13} photons s^{-1} at the ion source pressure of 10^{-4} mbar.[22]

dx.doi.org/10.1021/ac200742r |*Anal. Chem.* 2011, 83, 5309–5316

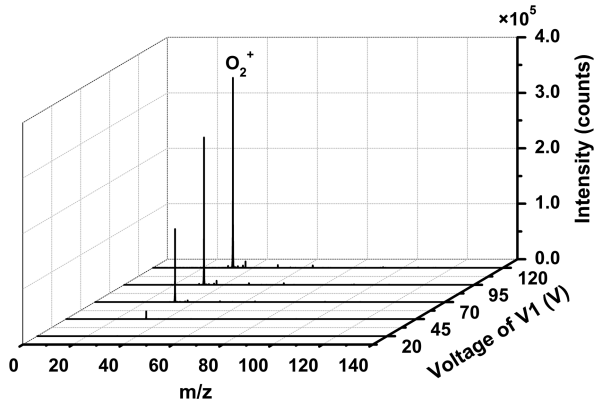

Figure 5. Three-dimensional plot for the SPI-CI mass spectra of the O_2^+ reactant ions from pure oxygen gas at different voltages of V1, 20, 45, 70, 95, and 120 V.

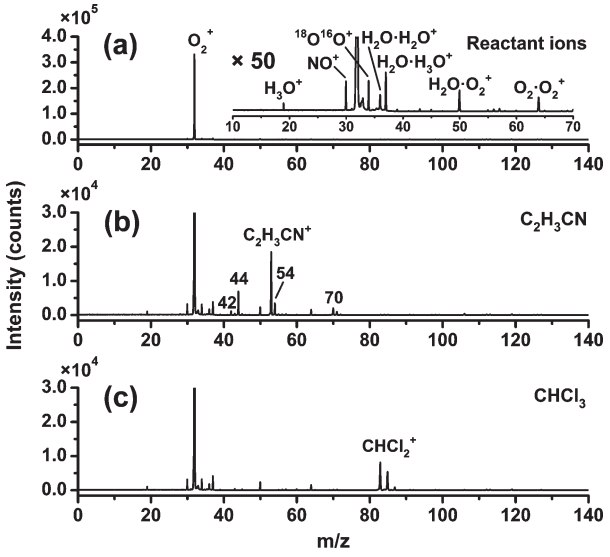

Figure 6. (a) SPI-CI mass spectrum of the reactant ions from pure oxygen gas. (b) SPI-CI mass spectrum of 10 ppmv propenenitrile (C_2H_3CN) gas sample. (c) SPI-CI mass spectrum of 10 ppmv chloroform ($CHCl_3$) gas sample.

Characteristics of SPI-CI Mode. In SPI-CI mode, pure oxygen gas was introduced into the ionization region between SE1 and SE2 as the reagent gas. The partial pressure of O_2 gas was measured at 0.2 mbar. The wavelength of the VUV radiation from the krypton discharge lamp is 116.5 nm (10.6 eV), which lies in a diffuse absorption band of O_2 (102−130 nm), and the absorption band at 116.1 nm of O_2 has been well reported previously.[42−44] Therefore, O_2 molecules in the ionization region will absorb the VUV radiation, and the efficiency of SPI could be reduced. However, the signal intensity of the analyte with the reagent gas of O_2 was only about 12% lower than that with the reagent gas of N_2 (Supporting Information, Figure S-1), as the partial pressure of O_2 gas in the ionization region was only 0.2 mbar. The VUV absorption of O_2 did not have a significant adverse effect on the efficiency of SPI. The reagent gas of NO was also used to generate NO^+ reactant ions in SPI-CI mode (Supporting Information, Figure S-2). For the detection of organic compounds in atmospheric samples, the presence of O_2 in the ionization region is inevitable in the direct-sampling MS system. Thus, O_2 was selected as the reagent gas in this study.

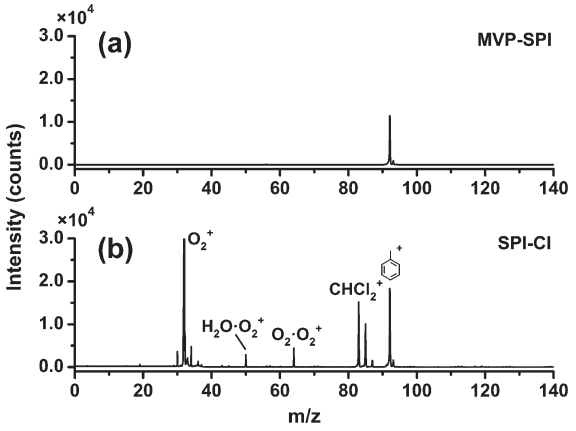

Figure 7. Mass spectra of a toluene and chloroform gas mixture with a respective concentration of 10 ppmv in different operation modes: (a) MVP-SPI mode; (b) SPI-CI mode.

Figure 5 illustrates the SPI-CI mass spectra of the O_2^+ reactant ions obtained at different voltages of V1. The yield of O_2^+ rose rapidly as the voltage of V1 increased, because the photoelectrons emitting from SE2 could obtain more energy to ionize O_2 molecules at higher electric fields in the ionization region between SE1 and SE2. The optimized voltage of V1 was found to be 120 V, and higher voltages of V1 would increase the risk of discharge in the ion source and saturation of the MCP detector.

The mass spectrum of pure oxygen gas in SPI-CI mode also contained some other ions such as H_3O^+, NO^+, and $H_2O \cdot O_2^+$, as shown in Figure 6a. These interfering ions will not affect the analysis performance of CI, because the intensities of these interfering ions are approximately 2 orders of magnitude lower than that of the O_2^+ reactant ions. Similar results were also found in the selected ion flow tube mass spectrometry (SIFT-MS).[45] The SPI-CI mass spectra of 10 ppmv propenenitrile (C_2H_3CN, IE = 10.91 eV)[33] and 10 ppmv chloroform ($CHCl_3$, IE = 11.37 eV)[33] gas samples are shown in parts b and c, respectively, of Figure 6. Production ions were also observed at m/z 42, 44, 54, and 70 besides the propenenitrile molecular ion ($C_2H_3CN^+$), while only the fragment ion peaks of $CHCl_2^+$ were observed at m/z 83, 85, and 87, owing to the isotope of ^{35}Cl and ^{37}Cl for chloroform. Compared to the EI mass spectra of propenenitrile and chloroform from NIST, the number of peaks in the SPI-CI mass spectra was dramatically reduced, which would make rapid qualitative and quantitative analysis more convenient. The O_2^+ reactant ions can effectively ionize not only propenenitrile and chloroform but also many other organic compounds, such as aldehydes, ketones, esters, and volatile carboxylic acids.[46,47]

In SPI-CI mode, the analyte molecules with IEs higher than 10.6 eV are ionized by CI, while others are ionized by both SPI and CI. The mass spectra of a 10 ppmv toluene and chloroform gas mixture in both MVP-SPI and SPI-CI modes are shown in parts a and b, respectively, of Figure 7. The peak intensity of toluene in SPI-CI mode was about 60% higher than that in MVP-SPI mode, which is the result of the higher ionization efficiency of toluene by both SPI and ion−molecule reactions in SPI-CI mode. However, the baseline noise in SPI-CI mode was almost three times higher than that in SPI mode because of the penetration of O_2^+ from the extraction region to the analyzer

dx.doi.org/10.1021/ac200742r |*Anal. Chem.* 2011, 83, 5309–5316

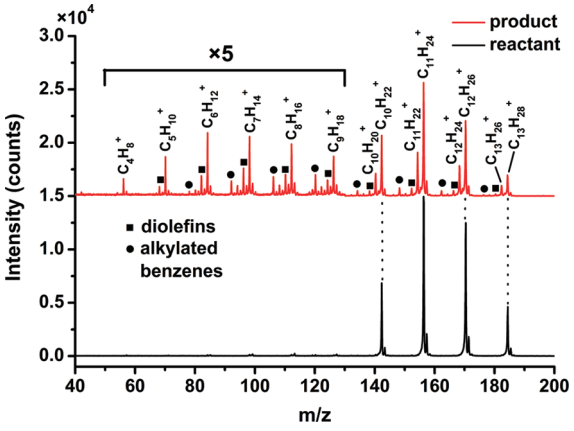

Figure 8. MVP-SPI mass spectra of the C10−C13 paraffins reactant and its dehydrogenation product.

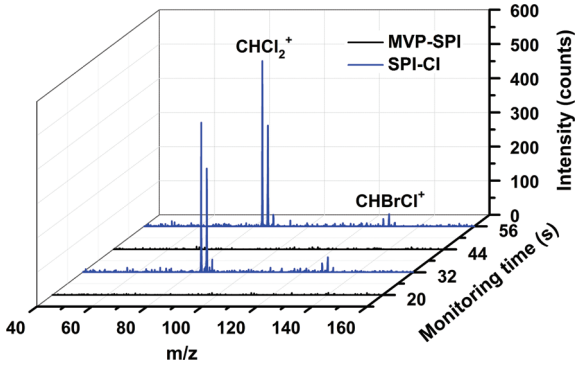

Figure 9. Three-dimensional plot of the MVP-SPI and SPI-CI mass spectra for continuous monitoring of organic compounds in disinfected drinking water.

during extraction pulses. Therefore, even with the 60% higher intensity obtained in SPI-CI mode for toluene, the LOD (S/N = 3) of toluene was 8 ppbv, which was a little worse than that in MVP-SPI mode (4 ppbv). The LOD for chloroform was found to be 10 ppbv in SPI-CI mode. Compared with the CI mode alone using commercial MS instruments, the SPI-CI mode of the combined ion source developed in this work has several advantages. First, more kinds of reagent gases can be used in SPI-CI mode, including various oxidizing gases, such as O_2 and NO, since there is not any heated filament in the combined ion source. Second, qualitative analysis of the mass spectra in SPI-CI mode can be more rapid and precise with the supplementary information from SPI. However, the intensity of the reactant ions in SPI-CI mode of the combined ion source is much lower than that in commercial CI-MS instruments because of the low light intensity of the VUV lamp used. This problem can be solved by utilizing VUV sources with higher light intensity.

Measurement of Complex Hydrocarbon Mixtures. Paraffins dehydrogenation for the production of the corresponding olefins is an important catalytic process in the oil industry.[48,49] MVP-SPI was used to monitor the C10−C13 paraffins mixture composition before and after dehydrogenation by Pt−Sn−K/Al_2O_3 catalyst. The liquid sample with a flow rate of 5 μL/min was heated to 200 °C to produce a gas sample and then was diluted with 1 L/min pure nitrogen. The diluted sample was transferred to the ion source through a heated transfer line (200 °C). The result is shown in Figure 8. The MVP-SPI mass spectrum of the mixture before dehydrogenation shows mainly four peaks corresponding to the molecular ions of C10−C13 paraffins. After catalytic dehydrogenation reactions, C10−C13 paraffins were partially converted to C10−C13 monoolefins and a small amount of byproduct was also identified in the dehydrogenation product, including some low molecular weight monoolefins, diolefins, and alkylated benzenes. In the previous study of the paraffins dehydrogenation process, the composition of the paraffins was analyzed by GC-MS,[49] while the diolefins content was analyzed with a gas chromatography-flame ionization detector (GC-FID) using a HP-FFAP column[50] or by high-performance liquid chromatography (HPLC) using a ZORBAX Rx-SIL column,[51] and the aromatics content was determined with a GC-FID using a HP-PONA column[50] or ultraviolet−visible (UV−vis) spectrophotometry.[51] The conversion efficiency of the dehydrogenation products was calculated by analyzing the bromine number.[49−51] The above analytical methods are laborious and time-consuming, which make it bothersome and difficult to realize online monitoring of the catalytic process. The MVP-SPI mass spectrometry can acquire the molecular weights of every constituent and their peak intensities within 10 s for qualitative and quantitative analysis, and it is appropriate for online and real-time detection of the organic product during the dehydrogenation reaction. It shows that MVP-SPI mass spectrometry has potential applications in the field of catalysis for reaction parameter optimization and catalyst performance evaluation.

Drinking Water Disinfection Byproducts Analysis. Disinfection of drinking water has made a tremendous contribution to public health. However, chlorine can react with the organic species in water to produce disinfection byproducts such as trihalomethanes (THMs), which include chloroform, bromodichloromethane, dibromochloromethane, and bromoform.[52,53] The new combined ion source can rapidly switch between MVP-SPI and SPI-CI modes, which are ideal for the analysis of drinking water disinfection byproducts from chlorine. To introduce analytes from the aqueous phase to the vacuum environment of the MS ion source, a membrane inlet was constructed to extract organic compounds.[17] A disinfected water sample was collected from piped water in our laboratory without pretreatment. Background mass spectra of the membrane inlet for both of the MVP-SPI and SPI-CI modes were acquired by introducing purified water before the measurement of the disinfected water sample. Figure 9 shows the mass spectra in MVP-SPI and SPI-CI modes separately for continuous monitoring of organic compounds in disinfected drinking water with a switching time of 2 s (this can be greatly reduced with modified electronics). Each mass spectrum was accumulated for 10 s with the background mass spectra subtracted. At 20 and 44 s, no ion was detected in MVP-SPI mode, which indicated that the concentrations of organic compounds with IEs lower than 10.6 eV in disinfected drinking water were beyond the LODs of this method. By contrast, $CHCl_2^+$ and $CHBrCl^+$ corresponding to chloroform ($CHCl_3$) and bromodichloromethane ($CHBrCl_2$, IE = 10.96 eV)[33] were able to be detected in SPI-CI mode at 32 and 56 s. The concentrations of $CHCl_3$ and $CHBrCl_2$ in piped water were found to be about 50 μg/L and 10 μg/L, respectively. It can be seen from the above experiment that the combination of the two ionization mechanisms expands the obtainable information considerably. In the previous study, the methods of GC using both electron capture and mass spectrometric detection were used for analysis of water disinfection byproducts.[53,54] However, sample pretreatment processes

involving liquid−liquid extraction, derivatization, or purge and trap are required prior to GC analysis. The coupling of the MVP-SPI/SPI-CI oaTOFMS with the membrane inlet can directly analyze water disinfection byproducts with a concentration of a few micrograms per liter in 10 s without any sample pretreatment, although the sensitivity is a little lower compared to that of GC methods. It is thought that the MVP-SPI/SPI-CI oaTOFMS system can be used as a rapid screening technique for disinfection byproducts in drinking water.

CONCLUSION

It has been demonstrated that the combined SPI and CI ion source with an oaTOFMS is a versatile analytical technique for monitoring complex organic mixtures with a wide range of IEs. The SPI sensitivity can be greatly improved by elevating the ion source pressure to medium vacuum pressure and lengthening the photoionization length, compared to the case of conventional high vacuum pressure SPI. In both MVP-SPI and SPI-CI modes, the LODs down to low-ppbv levels have been achieved for a number of aromatic and halogenated hydrocarbon compounds by directly introducing gas samples and using a commercial krypton discharge lamp. Similar to SPI, CI with O_2^+ reactant ions in SPI-CI mode is also characterized as a soft ionization technique by ionizing organic compounds without producing substantial fragmentation.

As the O_2^+ reactant ions for CI were generated by photoelectron ionization with pure oxygen, it can be easily changed to other reagent gases to generate different reactant ions by SPI, photoelectron ionization, or ion−molecule reactions at medium vacuum pressure. NO^+ reactant ions have already been successfully generated in the ionization region and used to ionize organic compounds (Supporting Information, Figure S-1). Future work will comprise swapping O_2^+ to other reactant ions, such as NH_4^+ and H_3O^+. Utilizing different reactant ions in SPI-CI mode is expected to improve the detection specificity and expand the detectable sample range.

It is likely that the MVP-SPI/SPI-CI oaTOFMS system has wide potential applications in online quality control, process monitoring, and real-time environmental analysis.

ASSOCIATED CONTENT

Supporting Information. Additional information as noted in the text. This material is available free of charge via the Internet at http://pubs.acs.org.

AUTHOR INFORMATION

Corresponding Author

*Fax: +86-411-84379517. E-mail: kyong.hou@gmail.com; hli@dicp.ac.cn.

ACKNOWLEDGMENT

Financial support from the National Natural Science Foundation of China (Grant Nos. 20877074, 20907052, and 40637036) and the Instrument Developing Project of the Chinese Academy of Sciences (Grant No. YZ200907) is gratefully acknowledged. The authors acknowledge Prof. Chenglin Sun of the Dalian Institute of Chemical Physics for providing the dehydrogenation samples.

REFERENCES

(1) Hanley, L.; Zimmermann, R. *Anal. Chem.* **2009**, *81*, 4174–4182.
(2) Saraj-Bozorgzad, M.; Geissler, R.; Streibel, T.; Muhlberger, F.; Sklorz, M.; Kaisersberger, E.; Denner, T.; Zimmermann, R. *Anal. Chem.* **2008**, *80*, 3393–3403.
(3) Pan, Y.; Zhang, L. D.; Zhang, T. C.; Guo, H. J.; Hong, X.; Qi, F. *J. Mass Spectrom.* **2008**, *43*, 1701–1710.
(4) Mitschke, S.; Welthagen, W.; Zimmermann, R. *Anal. Chem.* **2006**, *78*, 6364–6375.
(5) Muhlberger, F.; Streibel, T.; Wieser, J.; Ulrich, A.; Zimmermann, R. *Anal. Chem.* **2005**, *77*, 7408–7414.
(6) Shi, Y. J.; Lipson, R. H. *Can. J. Chem.* **2005**, *83*, 1891–1902.
(7) Kuribayashi, S.; Yamakoshi, H.; Danno, M.; Sakai, S.; Tsuruga, S.; Futami, H.; Morii, S. *Anal. Chem.* **2005**, *77*, 1007–1012.
(8) Mitschke, S.; Adam, T.; Streibel, T.; Baker, R. R.; Zimmermann, R. *Anal. Chem.* **2005**, *77*, 2288–2296.
(9) Schramm, E.; Kurten, A.; Holzer, J.; Mitschke, S.; Muhlberger, F.; Sklorz, M.; Wieser, J.; Ulrich, A.; Putz, M.; Schulte-Ladbeck, R.; Schultze, R.; Curtius, J.; Borrmann, S.; Zimmermann, R. *Anal. Chem.* **2009**, *81*, 4456–4467.
(10) Shi, Y. J.; Hu, X. K.; Mao, D. M.; Dimov, S. S.; Lipson, R. H. *Anal. Chem.* **1998**, *70*, 4534–4539.
(11) Tong, L.; Shi, Y. J. *J. Mass Spectrom.* **2010**, *45*, 215–222.
(12) Akhmetov, A.; Moore, J. F.; Gasper, G. L.; Koin, P. J.; Hanley, L. *J. Mass Spectrom.* **2010**, *45*, 137–145.
(13) Muhlberger, F.; Wieser, J.; Ulrich, A.; Zimmermann, R. *Anal. Chem.* **2002**, *74*, 3790–3801.
(14) Geissler, R.; Saraji-Bozorgzad, M. R.; Groger, T.; Fendt, A.; Streibel, T.; Sklorz, M.; Krooss, B. M.; Fuhrer, K.; Gonin, M.; Kaisersberger, E.; Denner, T.; Zimmermann, R. *Anal. Chem.* **2009**, *81*, 6038–6048.
(15) Li, J.; Cai, J. H.; Yuan, T.; Guo, H. J.; Qi, F. *Rapid Commun. Mass Spectrom.* **2009**, *23*, 1269–1274.
(16) Shi, Y. J.; Lo, B.; Tong, L.; Li, X.; Eustergerling, B. D.; Sorensen, T. S. *J. Mass Spectrom.* **2007**, *42*, 575–583.
(17) Hou, K. Y.; Wang, J. D.; Li, H. Y. *Rapid Commun. Mass Spectrom.* **2007**, *21*, 3554–3560.
(18) Wu, Q. H.; Hua, L.; Hou, K. Y.; Cui, H. P.; Chen, P.; Wang, W. G.; Li, J. H.; Li, H. Y. *Int. J. Mass Spectrom.* **2010**, *295*, 60–64.
(19) Mullen, C.; Irwin, A.; Pond, B. V.; Huestis, D. L.; Coggiola, M. J.; Oser, H. *Anal. Chem.* **2006**, *78*, 3807–3814.
(20) Streibel, T.; Weh, J. C.; Mitschke, S. *Anal. Chem.* **2006**, *78*, 5354–5361.
(21) Tsuruga, S.; Suzuki, T.; Takatsudo, Y.; Seki, K.; Yamuchi, S.; Kuribayashi, S.; Morii, S. *Environ. Sci. Technol.* **2007**, *41*, 3684–3688.
(22) Muhlberger, F.; Saraji-Bozorgzad, M.; Gonin, M.; Fuhrer, K.; Zimmermann, R. *Anal. Chem.* **2007**, *79*, 8118–8124.
(23) Muhlberger, F.; Wieser, J.; Morozov, A.; Ulrich, A.; Zimmermann, R. *Anal. Chem.* **2005**, *77*, 2218–2226.
(24) Syage, J. A.; Hanning-Lee, M. A.; Hanold, K. A. *Field Anal. Chem. Technol.* **2000**, *4*, 204–215.
(25) Syage, J. A.; Nies, B. J.; Evans, M. D.; Hanold, K. A. *J. Am. Soc. Mass Spectrom.* **2001**, *12*, 648–655.
(26) Nazarov, E. G.; Miller, R. A.; Eiceman, G. A.; Stone, J. A. *Anal. Chem.* **2006**, *78*, 4553–4563.
(27) Marchi, I.; Rudaz, S.; Veuthey, J. L. *Talanta* **2009**, *78*, 1–18.
(28) Robb, D. B.; Blades, M. W. *Anal. Chem.* **2006**, *78*, 8162–8164.
(29) Itoh, N.; Aoyagi, Y.; Yarita, T. *J. Chromatogr. A* **2006**, *1131*, 285–288.
(30) Mol, R.; de Jong, G. J.; Somsen, G. W. *Anal. Chem.* **2005**, *77*, 5277–5282.
(31) Hsieh, Y. S.; Merkle, K.; Wang, G. F. *Rapid Commun. Mass Spectrom.* **2003**, *17*, 1775–1780.
(32) Leinonen, A.; Kuuranne, T.; Kostiainen, R. *J. Mass Spectrom.* **2002**, *37*, 693–698.
(33) National Institute of Standards and Technology (NIST). http://webbook.nist.gov/chemistry.
(34) Wang, L.; Li, H. Y.; Bai, J. L.; Hua, X. Q.; Lu, R. C. *Int. J. Mass Spectrom.* **1998**, *181*, 43–50.
(35) Schriemer, D. C.; Li, L. *Anal. Chem.* **1996**, *68*, 250–256.
(36) Schriemer, D. C.; Li, L. *Rev. Sci. Instrum.* **1995**, *66*, 55–62.

(37) Colby, S. M.; Reilly, J. P. *Int. J. Mass Spectrom. Ion Processes* **1994**, *131*, 125–138.
(38) Cheng, P. Y.; Dai, H. L. *Rev. Sci. Instrum.* **1993**, *64*, 2211–2214.
(39) Muhlberger, F.; Zimmermann, R.; Kettrup, A. *Anal. Chem.* **2001**, *73*, 3590–3604.
(40) Gamez, G.; Zhu, L.; Schmitz, T. A.; Zenobi, R. *Anal. Chem.* **2008**, *80*, 6791–6795.
(41) Wiley, W. C.; McLaren, I. H. *Rev. Sci. Instrum.* **1955**, *26*, 1150–1157.
(42) Chang, H. C.; Ogawa, M. *J. Mol. Spectrosc.* **1972**, *44*, 405–406.
(43) England, J. P.; Lewis, B. R.; Gibson, S. T.; Ginter, M. L. *J. Chem. Phys.* **1996**, *104*, 2765–2772.
(44) Ogawa, M.; Yamawaki, K. R.; Hashizume, A.; Tanaka, Y. *J. Mol. Spectrosc.* **1975**, *55*, 425–429.
(45) Spanel, P.; Smith, D. *Int. J. Mass Spectrom.* **2009**, *280*, 128–135.
(46) Spanel, P.; Smith, D. *Int. J. Mass Spectrom.* **1998**, *172*, 137–147.
(47) Spanel, P.; Ji, Y. F.; Smith, D. *Int. J. Mass Spectrom.* **1997**, *165*, 25–37.
(48) He, S. B.; Sun, C. L.; Yang, X.; Wang, B.; Dai, X. H.; Bai, Z. W. *Chem. Eng. J.* **2010**, *163*, 389–394.
(49) He, S. B.; Sun, C. L.; Bai, Z. W.; Dai, X. H.; Wang, B. *Appl. Catal., A* **2009**, *356*, 88–98.
(50) He, S. B.; Sun, C. L.; Du, H. Z.; Dai, X. H.; Wang, B. *Chem. Eng. J.* **2008**, *141*, 284–289.
(51) Dai, X. H.; Suo, J. S.; Duan, X.; Bai, Z. W.; Zhang, L. *J. Surfactants. Deterg.* **2008**, *11*, 111–115.
(52) Hasan, A.; Thacker, N. P.; Bassin, J. *Environ. Monit. Assess.* **2010**, *168*, 489–497.
(53) Mosteo, R.; Miguel, N.; Martin-Muniesa, S.; Ormad, M. P.; Ovelleiro, J. L. *J. Hazard. Mater.* **2009**, *172*, 661–666.
(54) Smith, E. M.; Plewa, M. J.; Lindell, C. L.; Richardson, S. D.; Mitch, W. A. *Environ. Sci. Technol.* **2010**, *44*, 8446–8452.